RSC Advances

PAPER

View Article Online
View Journal | View Issue

Check for updates

Cite this: *RSC Adv.*, 2020, **10**, 10904

Reversible four-color electrochromism triggered by the electrochemical multi-step redox of Cr-based metallo-supramolecular polymers†

Takefumi Yoshida, Yoshikazu Ninomiya and Masayoshi Higuchi *

Four color electrochromism (yellow, magenta, blue, and navy) has been achieved in Cr(III)-based metallo-supramolecular polymers (**polyCr**), which were synthesized by 1 : 1 complexation of Cr ions and 1,4-di [[2,2′:6′,2″-terpyridin]-4′-yl]benzene (L). The polymer structure was determined by X-ray absorption fine structure (XAFS) measurement and X-ray photoelectron spectroscopy (XPS). The molecular weight of **polyCr** was calculated as 3.2×10^7 Da using right angle light scattering (RALS). The EXAFS fitting indicated that the bond distances of Cr–N are 2.020 Å and 2.208 Å. A film of **polyCr** shows multi-color electrochromism (EC) or absorption: a sharp peak at 380 nm at 0 V *vs.* Ag/Ag^+ (yellow), a sharp peak at 510 nm and a broad peak at 800 nm at −0.6 V *vs.* Ag/Ag^+ (magenta), a broad peak at 610 nm and between 700–900 nm at −1.2 V *vs.* Ag/Ag^+ (blue), a broad peak between 450–900 nm at −1.8 V *vs.* Ag/Ag^+ (navy). The transmittances change (ΔT), the switching times for coloring and bleaching (T_c, T_b) and the coloration efficiency (η_c, η_b): [ΔT, (T_c, T_b), (η_c, η_b)] were [39.2%, (5.56 s, 1.39 s), (169 cm^2 C^{-1}, 230 cm^2 C^{-1})] at 510 nm between −0.6 and 0.2 V *vs.* Ag/Ag^+, [67.0%, (6.93 s, 2.52 s), (138 cm^2 C^{-1}, 172 cm^2 C^{-1})] at 610 nm between −1.2 and 0.2 V *vs.* Ag/Ag^+, [86.1%, (6.80 s, 3.03 s), (167 cm^2 C^{-1}, 134 cm^2 C^{-1})] at 780 nm between −1.8 and 0.2 V *vs.* Ag/Ag^+, respectively, during the cycles. The durability experiment indicates that **polyCr** shows an EC property for at least 100 cycles.

Received 22nd January 2020
Accepted 28th February 2020

DOI: 10.1039/d0ra00676a

rsc.li/rsc-advances

Open Access Article. Published on 17 March 2020. Downloaded on 2/17/2026 12:55:54 AM.
This article is licensed under a Creative Commons Attribution-NonCommercial 3.0 Unported Licence.

Introduction

Electrochromic (EC) materials have been studied in the fields of organic molecules,[1] inorganic materials,[2] organic polymers,[3] and metallo-supramolecular polymers (MSPs),[4] and also, EC materials such as WO_3 or NiO have been used for smart windows, EC display and anti-glare rear view mirrors.[5] Furthermore, multi-color EC materials have received much attention in applications for EC displays.

The MSPs, which are prepared by a 1 : 1 complexation of metal ions with ditopic organic ligands, are a new type of coordination polymers and have been investigated for EC properties,[6] ion conductivity,[7] and luminescence.[8] These properties greatly depend on the metal species included in the polymer. In particular, group 8 metal ions (M = Fe, Ru, Os ions) based MSPs (**polyM**) show clear EC, whereas **polyM(II)** show a deep color [or metal-to-ligand charge-transfer (MLCT) in the visible region (*e.g.*, Fe: purple at 600 nm)] and **polyM(III)** show a transparent color (or no absorption in visible region), and in addition, they have been studied for use in EC displays with high durability.[6a,c,d] In addition, multi-color EC display of MSPs has also been reported which use multi-component based MSPs.[6d,9] The multi-color EC display with mononuclear MSPs has also been reported (*e.g.*, use of a Co complex shows yellow, orange or black colors).[10]

The origin of the word "chromism" comes from the element chrome (Cr) which shows different colors depending on its oxidation state. It also has characteristic properties such as catalysis,[11] magnetism,[12] and toxicity.[13] Recently, Farran *et al.* have reported Cr complexes with terpyridine ligands, where the Cr complexes show various oxidation states and colors at various potentials in the solution (they also reported the electron transfer process with the Ru ion).[14] Although they mainly reported electrochemical and photo-induced reduction processes, this study reported the potential of a solid-state multi-color Cr-based EC material.

In this work, Cr-based MSPs ($[Cr(L)]_n(ClO_4)_{3n}$:**polyCr**, Fig. 1) (L: 1,4-di[[2,2′:6′,2″-terpyridin]-4′-yl]benzene ligand) were synthesized and then characterized by X-ray absorption fine structure (XAFS) measurements, X-ray photoelectron spectroscopy (XPS) and right angle light scattering (RALS). The multi-color (yellow, magenta, blue, navy) electrochromic properties of **polyCr** were measured using cyclic voltammetry (CV) and chronoamperometry (CA) techniques with spectroscopy.

Results and discussion

The $Cr(II)Cl_2$ (12 mg, 0.1 mmol) was added to a suspension of L (54 mg, 0.1 mmol) in 100 ml methanol under N_2. After 30 min of

Electronic Functional Macromolecules Group, National Institute for Materials Science (NIMS), Tsukuba 305-0044, Japan. E-mail: HIGUCHI.Masayoshi@nims.go.jp

† Electronic supplementary information (ESI) available. See DOI: 10.1039/d0ra00676a

This journal is © The Royal Society of Chemistry 2020

Open Access Article. Published on 17 March 2020. Downloaded on 2/17/2026 12:55:54 AM.
This article is licensed under a Creative Commons Attribution-NonCommercial 3.0 Unported Licence.

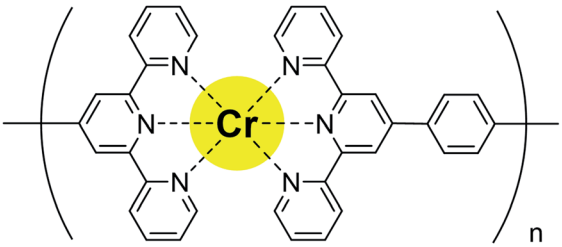

Fig. 1 The chemical structure of **polyCr**.

stirring, a purple solution was obtained. Next, the orange solution was obtained after 30 min of stirring under air [Cr(II) was oxidize to Cr(III)]. The solution filtered impurities an insoluble polymer. After the evaporation of the methanol, a yellow precipitate was obtained. The yellow precipitate was washed with a 0.1 M MeCN solution of $LiClO_4$ to exchange the counter anions (from Cl^- to ClO_4^-) and to the remove low molecular weight polymer. Finally, a yellow solid of **polyCr** was obtained. The molecular weight of **polyCr** was calculated as 3.2×10^7 Da using right angle light scattering (RALS), indicating the formation of MSPs. The results shown by the XPS spectra and emission spectrum are discussed in the ESI.† The TGA curve of **polyCr** is shown in Fig. S8 (ESI†). This polymer was stable up to 270 °C except for the possible weight loss of the crystal solvent. Only 15 wt% loss was observed at 500 °C. A film of **polyCr** was prepared on ITO by spin coating it with 200 μml of a 5 mg ml^{-1} methanol solution of **polyCr**.

To estimate the coordination structure of **polyCr**, the X-ray absorption fine structure measurements at the K-edge of the Cr ion were obtained from the synchrotron facility (BL-12C KEK). The X-ray absorption near edge structure (XANES) spectra measured at the Cr K-edge are shown in Fig. 2a. The Cr K-edge spectra of a pellet of **polyCr** was almost not shifted from 6006 eV (white line of the standard sample of Cr_2O_3).[15] The results indicated that the oxidation state of the Cr ions of **polyCr** was trivalent. From the extended X-ray absorption fine structure (EXAFS) region, the fitting by using crystal structure of reported Cr complex[16] (Fig. 2b) revealed that the coordination lengths around the Cr ions Cr–N were 2.020 Å and 2.208 Å (*R*-factor; 1.37%, Table 1, EXAFS oscillation is shown in Fig. S1, ESI†).

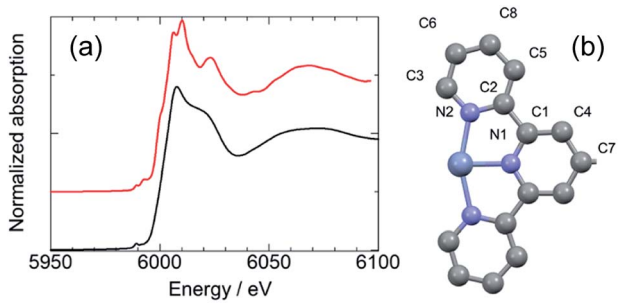

Fig. 2 (a) XANES spectra of a pellet of Cr_2O_3 (red curve) and **polyCr** (black curve), (b) asymmetry unit around the Cr ion of reported Cr complex.

These values were similar to the distances in the crystal structure. These results confirmed that the Cr ion of **polyCr** had an octahedral coordination structure.

The CVs of a cast film of **polyCr** were measured with a glassy carbon electrode (Fig. 3a). The sharp redox pairs (reduction, oxidation) of $[\mathbf{polyCr}]^{3+}/[\mathbf{polyCr}]^{2+}$, $[\mathbf{polyCr}]^{2+}/[\mathbf{polyCr}]^{+}$ were observed at (−0.55 V, −0.38 V) and (−0.91 V, −0.73) *vs.* Ag/Ag^+, respectively. These redox potentials were similar to those of reported Cr complexes. However, a large redox pair was observed at (−1.49 V, −1.08 V) *vs.* Ag/Ag^+. This peak can be assigned to the two electron transfers between $[\mathbf{polyCr}]^{+}/[\mathbf{polyCr}]^{-}$.[15,17] The CV of a film of **polyCr** was measured on ITO (Fig. S4, ESI†). An additional irreversible peak was observed when compared to CV on glassy carbon. This peak was from the reduction of ITO.

The transmittance spectrum of **polyCr** at various potentials is shown in Fig. 3b (images of **polyCr** at various potential are shown in Fig. 3c). There was a peak at 380 nm which was assigned to an intra ligand charge transfer transition (ILCT) at 0 V *vs.* Ag/Ag^+. As soon as the potential at −0.6 V *vs.* Ag/Ag^+ was applied, a sharp peak at 510 nm and a broad peak at 800 nm appeared. At −1.2 V *vs.* Ag/Ag^+, a sharp peak at 610 nm and a broad peak between 700–900 nm appeared. At −1.8 V *vs.* Ag/Ag^+, a broad peak between 450–900 nm appeared. These behaviours were similar to those reported for the solution of the Cr complex.[14] The color of the polymer film at each potential was defined, using the CIE 1964 XY color system, as 0.0 V: (0.36, 0.36), −0.6 V: (0.36, 0.33), −1.2 V: (0.29, 0.30), and −1.8 V: (0.26, 0.28) (Fig. 3d). From these results, a multi-color and wide-absorption solid-state EC material was made.

The transmittances in the colored and bleached states were 81.1% and 41.9% (ΔT = 39.2%) at 520 nm between −0.6 and 0.2 V *vs.* Ag/Ag^+, 91.1% and 24.1% (ΔT = 67.0%) at 610 nm between −1.2 and 0.2 V *vs.* Ag/Ag^+, and 98.1% and 12.0% (ΔT = 86.1%) at 780 nm between −1.8 and 0.2 V *vs.* Ag/Ag^+, during the cycles shown in Fig. 4a–c, respectively. These values were larger than those of previously reported MSPs (*e.g.*, **polyFe**: ΔT = ~55%).[6a] The switching times for coloring and bleaching (T_c and T_b) were 5.56 s and 1.39 s for 510 nm, 6.93 s and 2.52 s for 610 nm and 6.80 s and 3.03 s for 780 nm, respectively. These values were longer than those of previously reported MSPs (*e.g.*, **polyFe**: T_c: 0.37 s and T_b: 0.60 s).[6a] The coloration efficiency (η),

Table 1 Coordination distances of **polyCr** around the Cr ion

R-factor: 0.86%	*N*	*R*/Å	R_{eff}	Δ
N1	2	2.020	1.969	0.0503
N2	4	2.208	2.055	0.1528
C1	4	3.036	2.886	0.1501
C2	4	2.953	2.911	0.0426
C3	4	3.060	3.051	0.0086
C4	4	4.083	4.187	−0.1035
C5	4	4.245	4.235	0.0099
C6	4	4.376	4.344	0.03242
C7	2	4.711	4.725	−0.0138
C8	4	4.915	4.814	0.1010

Open Access Article. Published on 17 March 2020. Downloaded on 2/17/2026 12:55:54 AM.
This article is licensed under a Creative Commons Attribution-NonCommercial 3.0 Unported Licence.

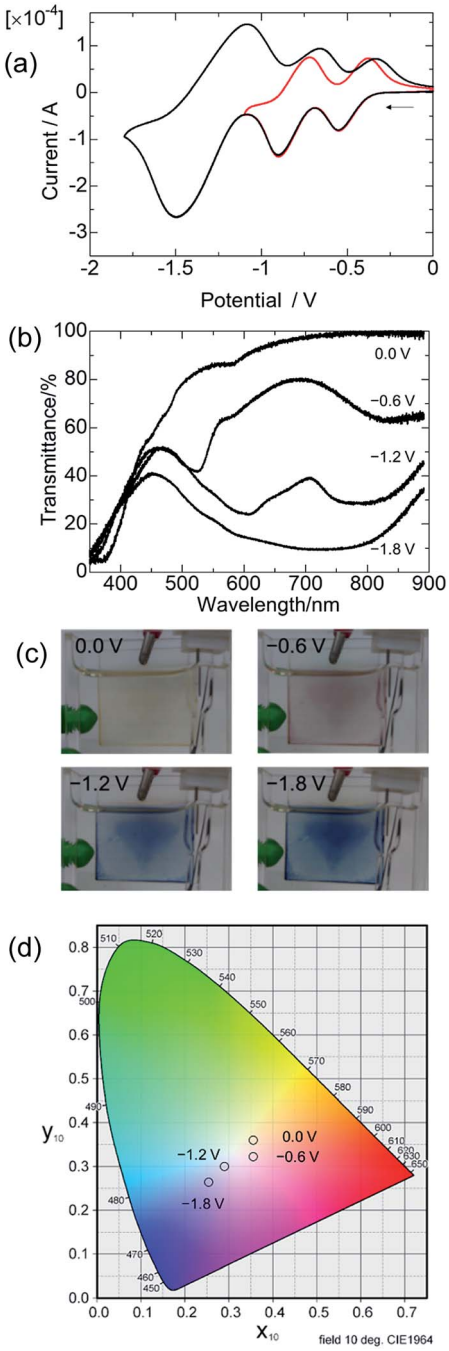

Fig. 3 (a) Cyclic voltammograms (CVs) of a cast film of **polyCr** on a glassy carbon electrode with a 0.1 M MeCN solution of $LiClO_4$ as electrolyte at a scan rate of 0.1 V s^{-1} (reference electrode: Ag/Ag^+), (b) transmittance spectrum of a film of **polyCr** on an ITO glass at various potentials, (c) images of the **polyCr** film on an ITO glass at various potentials, (d) CIE 1964 XY color system for each potential.

was used for evaluating the energy consumption, which was calculated using the following equation:[18]

$$\eta = \Delta OD/Q_d = \log(T_b/T_c)/Q_d \quad (1)$$

where η (cm^2 C^{-1}) is the coloration efficiency at a given ΔOD, and T_b and T_c are the transmittance values corresponding to the bleached and colored states, respectively. The Q_d was calculated as (1.69 mC cm^{-2}, 1.25 mC cm^{-2}) at 520 nm, (4.18 mC cm^{-2}, 3.34 mC cm^{-2}) at 610 nm, and (5.46 mC cm^{-2}, 6.80 mC cm^{-2}) at 780 nm from the current change as a function of time while applying the potential (Fig. 4d–f). The η (oxidation, reduction) were calculated as (169 cm^2 C^{-1}, 230 cm^2 C^{-1}) at 520 nm, (138 cm^2 C^{-1}, 172 cm^2 C^{-1}) at 610 nm, and (167 cm^2 C^{-1}, 134 cm^2 C^{-1}) at 780 nm, respectively. The η of reduction are higher than those of oxidation at 520 nm and 610 nm, because the sum of the leakage current is proportional to switching time. The η of reduction were lower than that of oxidation at 780 nm because the reduction current of ITO was included. Each η value was similar to that reported for the Fe and Ru polymers.[6a,d]

To confirm the durability of the color change, the repeated transmittance changes at 780 nm during the redox-switching between two potentials (−1.8 and 0.2 V) up to 100 cycles were monitored (Fig. 5). The transmittances in the colored states were constant at 12.0%, whereas those in the bleached states were slightly decreased (3%) during the cycles. This decrement was induced by a deterioration of ITO. In addition, the more cycles the EC system undergoes, the more current was observed because of the increase of the leakage current, which was induced by the deterioration of ITO (Fig. S5, ESI†). In other words, the durability of the electrochromic system can easily be improved by preventing the deterioration of ITO.

To investigate the film-forming properties of **polyCr**, the surface morphology of **polyCr** was measured by scanning electron microscopy (SEM), where a film was prepared by drop-casting. The SEM images of **polyCr** on ITO are shown in Fig. 6. The **polyCr** formed an almost flat surface. In addition, a fibrous structure was observed along the edge of the film.

Conclusions

A multi-color-electrochromic Cr(III)-based metallo-supramolecular polymer (**polyCr**) was synthesized by complexation of a Cr ion and 1,4-di[[2,2′:6′,2″-terpyridin]-4′-yl]benzene (L). The polymer structure was determined by XAFS spectroscopy measurement and XPS. The molecular weight of **polyCr** was calculated as 3.2 × 10^7 Da by RALS. The EXAFS fitting indicated that the bond distances of Cr–N were 2.020 Å and 2.208 Å. A film of **polyCr** shows electrochromism (EC) or absorption: a sharp peak at 380 nm at 0 V *vs.* Ag/Ag^+, a sharp peak at 510 nm and a broad peak at 800 nm at −0.6 V *vs.* Ag/Ag^+, a broad peak at 610 nm and between 700–900 nm at −1.2 V *vs.* Ag/Ag^+, a broad peak between 450–900 nm at −1.8 V *vs.* Ag/Ag^+. The transmittance changes (ΔT), the switching times for coloring and bleaching (T_c, T_b) and the coloration efficiency (η_c, η_b): [ΔT, (T_c, T_b), (η_c, η_b)] were [39.2%, (5.56 s, 1.39 s), (169 cm^2 C^{-1}, 230 cm^2 C^{-1})] at 510 nm between −0.6 and 0.2 V *vs.* Ag/Ag^+, [67.0%, (6.93 s, 2.52 s), (138 cm^2 C^{-1}, 172 cm^2 C^{-1})] at 610 nm between −1.2 and 0.2 V *vs.* Ag/Ag^+, [86.1%, (6.80 s, 3.03 s), (167 cm^2 C^{-1}, 134 cm^2 C^{-1})] at 780 nm between −1.8 and 0.2 V *vs.* Ag/Ag^+, respectively, during the cycles. The durability experiment indicated that **polyCr** shows an EC property for at

 This journal is © The Royal Society of Chemistry 2020

Open Access Article. Published on 17 March 2020. Downloaded on 2/17/2026 12:55:54 AM.
This article is licensed under a Creative Commons Attribution-NonCommercial 3.0 Unported Licence.

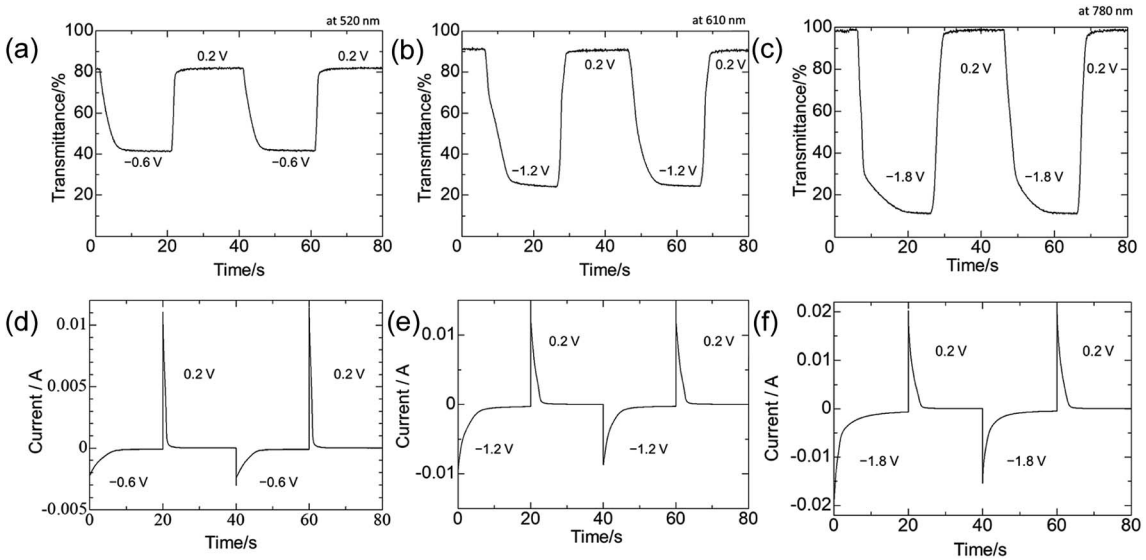

Fig. 4 Transmittance/current *vs.* time plots of a film of **polyCr** (a) and (d) at 520 nm between −0.6 and 0.2 V *vs.* Ag/Ag^+, (b) and (e) at 610 nm between −1.2 and 0.2 V *vs.* Ag/Ag^+, (c) and (f) at 780 nm between −1.8 and 0.2 V *vs.* Ag/Ag^+.

least 100 cycles. These properties are important for the fabrication of EC devices.

Experimental

Synthesis of polyCr

The Cr(II)Cl_2 (12 mg, 0.1 mmol) was added to a suspension of L (54 mg, 0.1 mmol) in 100 ml of methanol under N_2. After 30 min of stirring, a purple solution was obtained. Next, an orange solution was obtained after 30 min of stirring under air [Cr(II) was oxidized to Cr(III)]. The solution filtered impurities an insoluble polymer. After evaporation of the methanol, a yellow precipitate was obtained. The yellow precipitate was washed with a 0.1 M MeCN solution of $LiClO_4$ to exchange the counter anion (from Cl^- to ClO_4^-) and to remove low molecular weight polymer. Finally, a yellow solid of **polyCr** of was obtained. A film of **polyCr** (working area 2 cm × 2.5 cm) on ITO (8 Ω sq^{-1}, 2.5 cm × 2.5 cm) was prepared by a spin coating method with 200 μml of a 5 mg ml^{-1} methanol solution of **polyCr**. The HR-MS results were: found *m*/*z*: 628.23 [M + L + Cl] and 663.16 [M + L + 2Cl]; calcuation *m*/*z*: 628.12 [M + L + Cl] ($C_{35}H_{26}N_6ClCr$) and 663.09 [M + L + 2Cl] ($C_{35}H_{26}N_6Cl_2Cr$) (Fig. S6, ESI†). The IR spectrum results [Fig. S7, (ESI†) cm^{-1}]: 3353 (s), 3064 (s), 1615 (s), 1465 (s), 1242 (m), 1093 (m), 1031 (m), 795 (m), 530 (br).

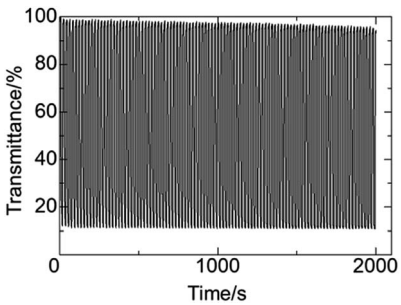

Fig. 5 The repeated transmittance changes at 780 nm during the redox-switching between two potentials (−1.8 and 0.2 V) up to 100 cycles.

Spectroscopy

X-ray absorption fine structure (XAFS) measurements were carried out at the BL12C beamline of the Photon Factory, the High Energy Accelerator Research Organization (KEK), under proposal no. 2019G117. Structural analysis was performed using the Demeter software platform. The reported crystal data was used for calculating F_{eff}. The FT-IR spectra were acquired on a FTIR-8400S infrared spectrophotometer (Shimadzu). The UV-vis spectra were acquired on an Ocean spectrometer (Ocean Insight). Solid state emission spectra were acquired on a RF-5300PC spectrofluorophotometer (Shimadzu). The RALS was recorded in methanol solution, on a 270 Dual Detector (Viscotek). The XPS was performed on an Axis Nova (Kratos Analytical, Al Kα = 1.4866 keV).

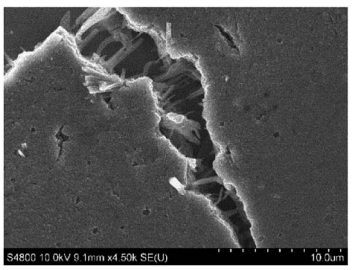

Fig. 6 SEM image of **polyCr** on ITO.

Open Access Article. Published on 17 March 2020. Downloaded on 2/17/2026 12:55:54 AM.
This article is licensed under a Creative Commons Attribution-NonCommercial 3.0 Unported Licence.

Electrochemistry

The CV and CA were performed on a electrochemical workstation (CH Instruments Inc., ALS/CHI) with a three-electrode system (polymer-coated ITO glass substrate and a glassy carbon working electrode, platinum wire as the counter electrode, and $Ag/AgNO_3$ as the reference electrode).

Conflicts of interest

There are no conflicts to declare.

Acknowledgements

This research is financially supported by the JST-CREST project (grant number: JPMJCR1533). This work was conducted at the AIST Nano-Processing Facility, supported by "Nanotechnology Platform Program" of the Ministry of Education, Culture, Sports, Science and Technology (MEXT), Japan. The X-ray absorption fine structure was collected on the BL-12C beamline in the Photon Factory of the High Energy Accelerator Research Organization (KEK, proposal no. 2019G117).

Notes and references

1 (*a*) Y.-M. Zhang, X. Wang, W. Zhang, W. Li, X. Fang, B. Yang, M. Li and S. X.-A. Zhang, *Light: Sci. Appl.*, 2015, **4**, e249; (*b*) A. Hein, C. Kortz and E. Oesterschulze, *Sci. Rep.*, 2019, **9**, 15822; (*c*) A. N. Woodward, J. M. Kolesar, S. R. Hall, N.-A. Saleh, D. S. Jones and M. G. Walter, *J. Am. Chem. Soc.*, 2017, **139**, 8467–8473.

2 (*a*) G. Gao, L. Xu, W. Wang, W. An and Y. Qiu, *J. Mater. Chem.*, 2004, **14**, 2024–2029; (*b*) C. G. Granqvist, M. A. Arvizu, İ. Bayrak Pehlivan, H. Y. Qu, R. T. Wen and G. A. Niklasson, *Electrochim. Acta*, 2018, **259**, 1170–1182; (*c*) G. Cai, J. Wang and P. S. Lee, *Acc. Chem. Res.*, 2016, **49**, 1469–1476; (*d*) G. Cai, P. Darmawan, M. Cui, J. Wang, J. Chen, S. Magdassi and P. S. Lee, *Adv. Energy Mater.*, 2016, **6**, 1501882; (*e*) L. Shen, L. Du, S. Tan, Z. Zang, C. Zhao and W. Mai, *Chem. Commun.*, 2016, **52**, 6296–6299; (*f*) R.-T. Wen, C. G. Granqvist and G. A. Niklasson, *Nat. Mater.*, 2015, **14**, 996–1001; (*g*) C. Yan, W. Kang, J. Wang, M. Cui, X. Wang, C. Y. Foo, K. J. Chee and P. S. Lee, *ACS Nano*, 2014, **8**, 316–322; (*h*) E. L. Runnerstrom, A. Llordés, S. D. Lounis and D. J. Milliron, *Chem. Commun.*, 2014, **50**, 10555–10572; (*i*) H. S. Chavan, B. Hou, A. T. A. Ahmed, Y. Jo, S. Cho, J. Kim, S. M. Pawar, S. Cha, A. I. Inamdar, H. Im and H. Kim, *Sol. Energy Mater. Sol. Cells*, 2018, **185**, 166–173.

3 (*a*) T.-H. Chang, H.-C. Lu, M.-H. Lee, S.-Y. Kao and K.-C. Ho, *Sol. Energy Mater. Sol. Cells*, 2018, **177**, 75–81; (*b*) İ. Yağmur, M. Ak and A. Bayrakçeken, *Smart Mater. Struct.*, 2013, **22**, 115022; (*c*) H. Wei, J. Zhu, S. Wu, S. Wei and Z. Guo, *Polymer*, 2013, **54**, 1820–1831; (*d*) W.-H. Wang, J.-C. Chang and T.-Y. Wu, *Org. Electron.*, 2019, **74**, 23–32; (*e*) T. An, Y. Ling, S. Gong, B. Zhu, Y. Zhao, D. Dong, L. W. Yap, Y. Wang and W. Cheng, *Adv. Mater. Technol.*, 2019, **4**.

4 M. Lahav and M. E. v. d. Boom, *Adv. Mater.*, 2018, **30**.

5 (*a*) Y. Wang, E. L. Runnerstrom and D. J. Milliron, *Annu. Rev. Chem. Biomol. Eng.*, 2016, **7**, 283–304; (*b*) V. K. Thakur, G. Ding, J. Ma, P. S. Lee and X. Lu, *Adv. Mater.*, 2012, **24**, 4071–4096; (*c*) X. Li, K. Perera, J. He, A. Gumyusenge and J. Mei, *J. Mater. Chem. C*, 2019, **7**, 12761–12789; (*d*) H.-J. Yen and G.-S. Liou, *Polym. Chem.*, 2018, **9**, 3001–3018.

6 (*a*) C.-W. Hu, T. Sato, J. Zhang, S. Moriyama and M. Higuchi, *ACS Appl. Mater. Interfaces*, 2014, **6**, 9118–9125; (*b*) B.-H. Chen, S.-Y. Kao, C.-W. Hu, M. Higuchi, K.-C. Ho and Y.-C. Liao, *ACS Appl. Mater. Interfaces*, 2015, **7**, 25069–25076; (*c*) M. K. Bera, C. Chakraborty, U. Rana and M. Higuchi, *Macromol. Rapid Commun.*, 2018, **39**, 1800415; (*d*) C.-W. Hu, T. Sato, J. Zhang, S. Moriyama and M. Higuchi, *J. Mater. Chem. C*, 2013, **1**, 3408–3413.

7 (*a*) R. K. Pandey, U. Rana, C. Chakraborty, S. Moriyama and M. Higuchi, *ACS Appl. Mater. Interfaces*, 2016, **8**, 13526–13531; (*b*) R. K. Pandey, M. Delwar Hossain, C. Chakraborty, S. Moriyama and M. Higuchi, *Chem. Commun.*, 2015, **51**, 11012–11014; (*c*) R. K. Pandey, M. D. Hossain, T. Sato, U. Rana, S. Moriyama and M. Higuchi, *RSC Adv.*, 2015, **5**, 49224–49230.

8 (*a*) Y. Zhou, H.-Y. Zhang, Z.-Y. Zhang and Y. Liu, *J. Am. Chem. Soc.*, 2017, **139**, 7168–7171; (*b*) L. Babel, L. Guenee, C. Besnard, S. V. Eliseeva, S. Petoud and C. Piguet, *Chem. Sci.*, 2018, **9**, 325–335; (*c*) D. Yang, Y. Wang, D. Liu, Z. Li and H. Li, *J. Mater. Chem. C*, 2018, **6**, 1944–1950; (*d*) T. Sato, R. K. Pandey and M. Higuchi, *Dalton Trans.*, 2013, **42**, 16036–16042; (*e*) P. Chen, Q. Li, S. Grindy and N. Holten-Andersen, *J. Am. Chem. Soc.*, 2015, **137**, 11590–11593.

9 Y. Kuai, W. Li, Y. Dong, W.-Y. Wong, S. Yan, Y. Dai and C. Zhang, *Dalton Trans.*, 2019, **48**, 15121–15126.

10 C.-Y. Hsu, J. Zhang, T. Sato, S. Moriyama and M. Higuchi, *ACS Appl. Mater. Interfaces*, 2015, **7**, 18266–18272.

11 (*a*) S. E. Denmark and J. Fu, *Chem. Rev.*, 2003, **103**, 2763–2794; (*b*) M. Bandini, P. G. Cozzi and A. Umani-Ronchi, *Tetrahedron*, 2001, **57**, 835–843.

12 (*a*) D. A. Cummings, J. McMaster, A. L. Rieger and P. H. Rieger, *Organometallics*, 1997, **16**, 4362–4368; (*b*) F. Moro, D. Kaminski, F. Tuna, G. F. S. Whitehead, G. A. Timco, D. Collison, R. E. P. Winpenny, A. Ardavan and E. J. L. McInnes, *Chem. Commun.*, 2014, **50**, 91–93; (*c*) A. Ardavan, O. Rival, J. J. L. Morton, S. J. Blundell, A. M. Tyryshkin, G. A. Timco and R. E. P. Winpenny, *Phys. Rev. Lett.*, 2007, **98**, 057201; (*d*) J. H. Christian, D. W. Brogden, J. K. Bindra, J. S. Kinyon, J. van Tol, J. Wang, J. F. Berry and N. S. Dalal, *Inorg. Chem.*, 2016, **55**, 6376–6383; (*e*) M. S. Fataftah, J. M. Zadrozny, S. C. Coste, M. J. Graham, D. M. Rogers and D. E. Freedman, *J. Am. Chem. Soc.*, 2016, **138**, 1344–1348; (*f*) S. Lenz, H. Bamberger, P. P. Hallmen, Y. Thiebes, S. Otto, K. Heinze and J. van Slageren, *Phys. Chem. Chem. Phys.*, 2019, **21**, 6976–6983.

13 M. Owlad, M. K. Aroua, W. A. W. Daud and S. Baroutian, *Water, Air, Soil Pollut.*, 2009, **200**, 59–77.

 This journal is © The Royal Society of Chemistry 2020

Open Access Article. Published on 17 March 2020. Downloaded on 2/17/2026 12:55:54 AM.
This article is licensed under a Creative Commons Attribution-NonCommercial 3.0 Unported Licence.

14 R. Farran, L. Le-Quang, J.-M. Mouesca, V. Maurel, D. Jouvenot, F. Loiseau, A. Deronzier and J. Chauvin, *Dalton Trans.*, 2019, **48**, 6800–6811.
15 C. C. Scarborough, K. M. Lancaster, S. DeBeer, T. Weyhermüller, S. Sproules and K. Wieghardt, *Inorg. Chem.*, 2012, **51**, 3718–3732.
16 J. Schönle, E. C. Constable, C. E. Housecroft and M. Neuburger, *Inorg. Chem. Commun.*, 2015, **53**, 80–83.
17 M. C. Hughes and D. J. Macero, *Inorg. Chem.*, 1976, **15**, 2040–2044.
18 M. Higuchi, *J. Mater. Chem. C*, 2014, **2**, 9331–9341.